

STABILITY OF RAYLEIGH–BÉNARD CONVECTION ROLLS AND BIMODAL FLOW AT MODERATE PRANDTL NUMBER

JOHN A. WHITEHEAD Jr. * and GERALD L. CHAN **

Institute of Geophysics and Planetary Physics, U.C.L.A., Los Angeles, Calif. (U.S.A.)

School of Engineering and Applied Science, U.C.L.A., Los Angeles, Calif. (U.S.A.)

(Received January 5, 1976)

ABSTRACT

Whitehead Jr., J.A. and Chan, G.L., 1976. Stability of Rayleigh–Bénard convection rolls and bimodal flow at moderate Prandtl number. *Dyn. Atmos. Oceans*, 1: 33–49.

Experimental observations of cellular convection between two rigid, horizontal, conducting boundaries are reported for two different cases. First, the stability of two-dimensional roll convection of various wavenumbers and Rayleigh numbers is investigated in fluids of Prandtl numbers 16 and 2.7. The results qualitatively agree with earlier observations by Busse and Whitehead of fluid with Prandtl number 126 but they differ somewhat quantitatively. Second, the stability of the bimodal flow, consisting of two rolls of differing and perpendicular wavenumber, is observed to be stable for given bandwidths and ranges of Rayleigh numbers when the configuration of the bimodal flow, consisting of two sets of rolls at right angles, is flawless — without any disruptions in the periodic matrix. The stability range differs from earlier experiments and from our own experiments in which the bimodal planform is uncontrolled.

INTRODUCTION

From the time that the experiments of Bénard (1901) were first reported, it has been known that a horizontal layer of fluid heated from below exhibits strikingly simple geometrical convection patterns when the temperature difference is raised above a certain critical value. On the basis of observations of the change of slope of the heat flux vs. temperature, Malkus (1954) proposed that the convection liberated progressively more and more convection modes with increased temperature difference across the layer, and suggested that the convection system is an ideal subject for turbulence investigations because the progressive transitions can be investigated in detail. In the interior of the earth, in the ocean, and in the atmosphere, such convection occurs, often in a relatively structured manner, yet little is known of the details of how these structures come about.

* Present address, Department of Physical Oceanography, Woods Hole Oceanographic Institution, Woods Hole, Mass. (U.S.A.).

** Present address, Harvard School of Public Health, Boston, Mass. (U.S.A.).

Recent studies into the geometric form of convection confirm the consistency of Malkus' original hypothesis. Although the convection above the critical Rayleigh number consisted of two-dimensional roll-like cells, Busse (1967) showed theoretically that the roll-form of convection cannot exist above a Rayleigh number of approximately 22,000 because rolls at right angles grow. The flow was observed to become three-dimensional by Krishnamurti (1970a) and this transition was accompanied by a change in the slope of the heat-flux curve. The three-dimensional pattern was observed to consist of two sets of rolls lying at right angles and of different wavelength by Busse and Whitehead (1971), and this pattern has henceforth been called bimodal flow. Further studies by Krishnamurti (1970b) and by Willis and Deardorff (1970) reported a gradual transition to time-dependent flow in large Prandtl number fluid in the Rayleigh number range between 60,000 to somewhat over 100,000. Krishnamurti further observed accompanying changes in the heat-flux curve. Recent studies by Busse and Whitehead (1974) show a much clearer transition to a time-dependent flow when the geometry of bimodal flow is carefully controlled.

The purpose of the present paper is to report the results of further studies of the stability of convection rolls and bimodal flows for various Prandtl numbers, wavenumbers, and Rayleigh numbers. To this end we first describe observations of the stability of roll convection for silicon oil with a Prandtl number of 16 and hot water with a Prandtl number of 2.7 and such transitions have been observed by us to behave qualitatively like the transitions predicted by Busse for fluid with infinite Prandtl number, and observed by Busse and Whitehead (1971) in fluid with a Prandtl number of 126. Secondly, we investigate the stability of the bimodal flow for fluid with a Prandtl number of 126 and we find that the bimodal flow is stable in a given volume in Rayleigh number, and two wavenumber space.

To accomplish these observations the experimental technique of Chen and Whitehead (1968) was used to generate roll and bimodal convection consisting of parallel planar rolls of a specified wavelength as an initial condition. It was found that the instability of convection in a perfect bimodal planform, that is, one consisting of two sets of planar rolls at exactly right angles without any flaws in the bimodal matrix, has stability properties unlike those reported by Krishnamurti (1970b) or Willis and Deardorff (1970). It was found, however, that when the bimodal pattern was not "perfectly flawless," as is always the case when initial conditions of the convection are not controlled, a new convection pattern grew at the flaw regions, which appears to possess the oscillatory properties reported in the above papers. We believe that this is evidence that such an instability does not grow from background noise in the bimodal flow, and hence that a transition to oscillations will not be predicted by a linearized stability analysis in the ranges observed here.

THE EXPERIMENTAL APPARATUS

Two convection chambers of different sizes but similar designs were used in the present experiments. The larger chamber was used for Rayleigh numbers

above 10,000 in the $Pr = 16$ and the $Pr = 126$ case whereas the rest of the experiments were done with the smaller apparatus.

A schematic diagram of the larger apparatus is shown in Fig. 1. It consists of two water channels, one placed horizontally above the other at a precise spacing, thus leaving a middle channel in between the two, which is filled with the working fluid. The bottom channel has a dimension of $100 \times 91 \text{ cm}^2$ and is bounded by a one-half-inch-thick piece of plate glass below, and a one-quarter-inch piece of plate glass above. The top channel has a dimension of $80 \times 80 \text{ cm}^2$ and is bounded by one-quarter-inch-thick pieces of plate glass. It is held in place by four brass brackets at its four corners. Although glass has about 5.6 better heat conductivity than the silicon oil, and 1.5 better conductivity than water, there is no other material which has higher thermal conductivity and meets the requirements of transparency and economy.

In the water channels the circulating water is thermally regulated. The water in the two channels is drawn from two separate units of constant-temperature water baths which are capable of delivering up to five gallons of water per minute at any desired temperature between room temperature and 100°C . The thermostats in these baths maintain the water at a constant temperature to within a few hundredths of a degree Kelvin. Since the water in the two channels serves as the thermal boundary for the convection layer, it is essential that its flow be spatially homogeneous. A distributor is used both at the inlet and the outlet such that the flow may be as close as possible to being parallel. For the same reason, a rather high flow rate is employed, thus eliminating the possibility of a significant temperature gradient between the inlet and the outlet. The one-quarter-inch glass plates bounding the channels are not sufficient in strength to remain flat while supporting the weights of the fluids and their own weight. A counter pressure system is necessary to maintain the hydrostatic head in the lower, middle, and upper channels constant to 1 mm. To achieve this, water is pumped from each bath to a constant head reservoir from which it is introduced to the inlets of the channels. Spillways of adjustable height are placed at the outlets. Each fluid is maintained $3/8''$ deeper than the fluid above it to compensate for the weight of the $1/4''$ glass plates.

The whole apparatus is very carefully leveled to avoid any mean flow. The precise depth of the convecting layer is obtained by placing spacers of exact thickness at the four corners of the upper channel and adjusting the dial attached to each of the brackets supporting the upper channel. A layer depth of 4.0 mm and 5.5 mm was used respectively in the $Pr = 16$ and 2.7 experiments. A layer depth of 10, 15, and 20 mm was used respectively in the $Pr = 126$ experiments. The desired Rayleigh-number range prescribes the depth of the layer. Plexiglass bars milled to exact thickness are placed underneath the four sides of the upper channel to serve as lateral boundaries to the convection layer.

The optics of the apparatus are shown in Fig. 2. A slightly diverging beam of light emanates from a light source approximately 15 feet away. It is reflected upward by the lower mirror, traversing the fluid layers in its path. It

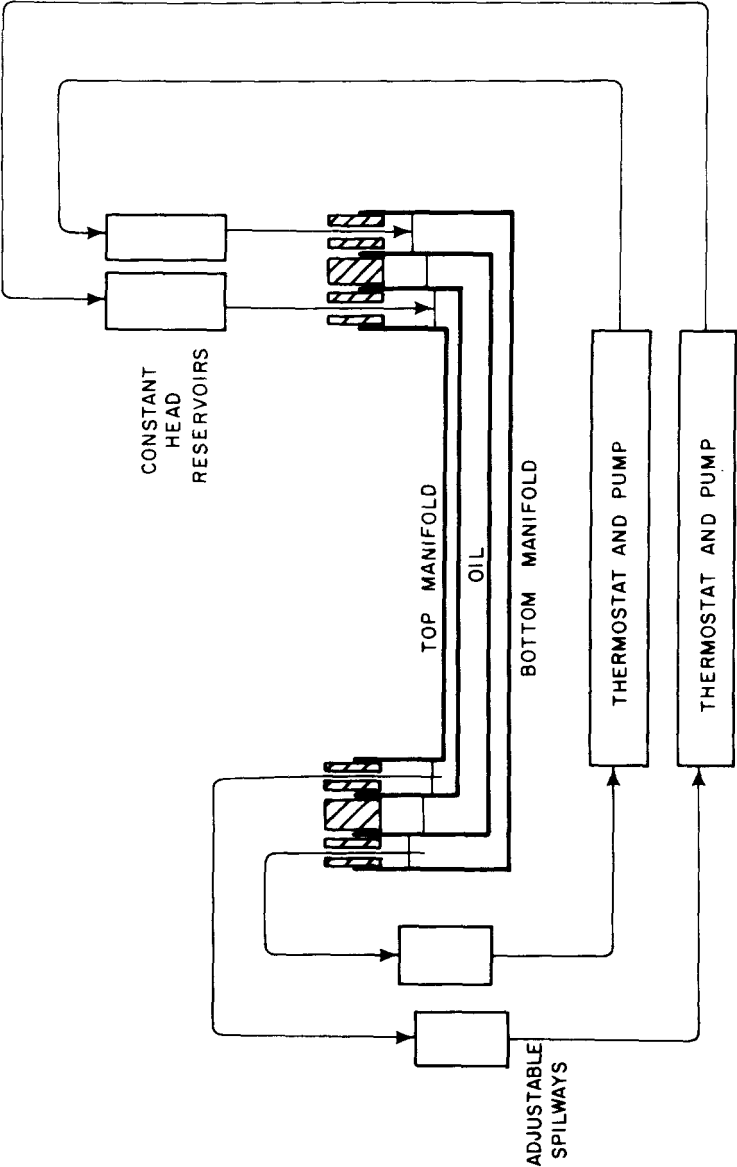


Fig. 1. Schematic diagram of the large experimental apparatus. Arrows indicate water flow. Heavy lines indicate glass, hashed regions indicate styrofoam insulation.

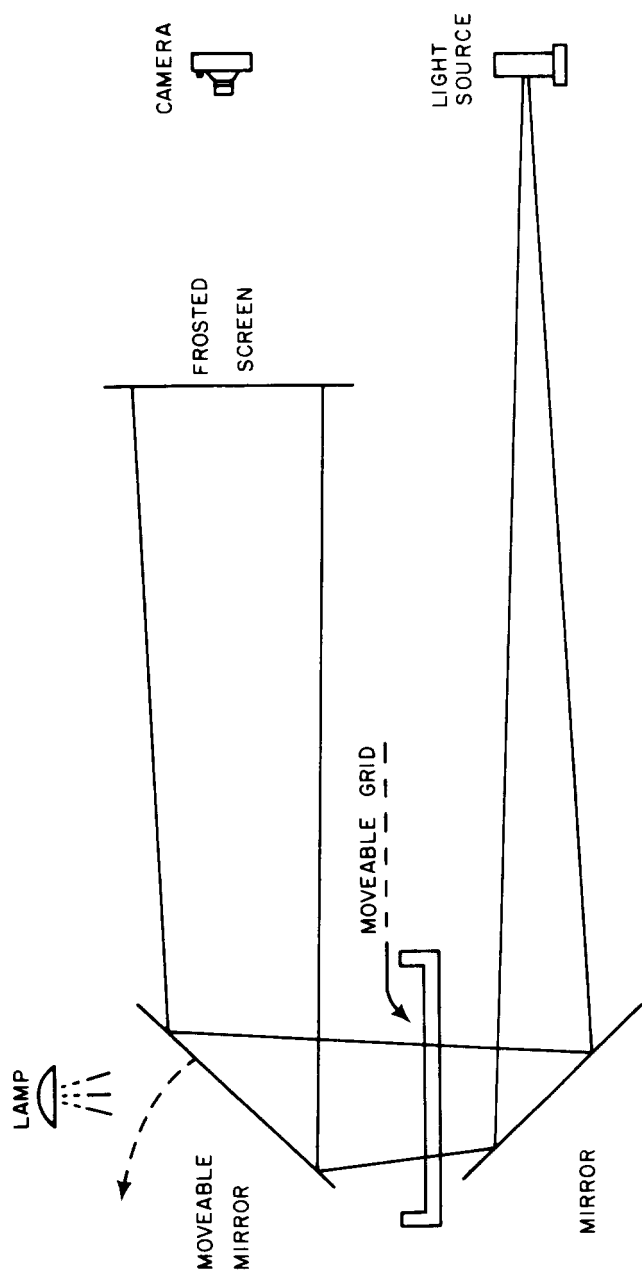


Fig. 2. Schematic diagram of the optics of the large apparatus.

is then reflected by the upper mirror onto a screen on which the convection patterns may be viewed. An ascending region in the convection layer has a smaller density and acts as a concave lens to the beam of light, thus producing a dark image on the screen. Conversely, the descending regions appear as bright lines on the screen.

The heat source for creating the initial perturbation are two 500-W light bulbs fixed at a distance of 1.5 m above the convection layer. The grids used in creating the periodicity in the initial perturbation are of the same size as the upper channel. They are made of aluminum frames with silver tapes mounted across them at exact spacings. The width of one tape plus the spacing to its adjacent tape constitute one wavelength.

The use of a smaller apparatus for some of the experiments is necessitated on two accounts. Firstly, in order to achieve Rayleigh numbers below 10,000 it is necessary to have a depth of 2.8 mm because of the inherent material properties of the $Pr = 16$ fluid. The thickness of the brackets supporting the upper channel renders this impossible. The same applies also to hot water in the whole range of Rayleigh numbers covered. Secondly, in the case of hot water, it is difficult to maintain a large amount of circulating water in the vicinity of 70°C.

The smaller convection chamber is basically the same as the larger one already described. It is contained in a plexiglass box $30 \times 30 \text{ cm}^2$. Instead of a bottom channel, it has an aluminum block with water circulating inside. A mirror is placed on top of that and the top glass channel rests on top of the mirror through four plexiglass strips milled to exact thickness which serve also as lateral boundaries. The circulating water baths are the same as described in the former case. The optical arrangement, however, differs slightly. An inclined mirror is placed on top of the convection layer which directs the beam of light downward and is reflected by the bottom mirror. In so doing, the light traverses twice through the convection layer, thus enhancing the contrasts. It is then projected by the top mirror to a screen where observations may be made.

The working fluids in the present experiments are two Dow Corning 200 silicone oils and hot water at 70°C. Their properties are shown in Table I.

Experimental procedure

The convection region is first held below the critical Rayleigh number for an interval of time equal to at least a few thermal time constants, d^2/K , of the oil, where d is depth of the fluid and K is thermal diffusivity. During this period, the grid consisting of regularly spaced tapes stretching across a frame is placed over the upper glass jacket, and the light is shone downward through the grid into the fluid. A small amount of this radiant energy is absorbed by the silicon oil in the illuminated regions, resulting in rows of slightly heated (0.05° K by direct measurement) oil spaced the desired distance apart. Next, the temperature of the top thermostatic bath is decreased, and that of the bottom bath is increased so that the Rayleigh number of oil is raised above

TABLE I.

Material properties of working fluids

	Kinematic viscosity at 25°C (centistokes)	Coefficient of expansion (°C ⁻¹)	Thermometric conductivity (cm ² /sec)	Prandtl number (<i>Pr</i>)
Silicone oil	10	$1.08 \cdot 10^{-3}$	$7.9 \cdot 10^{-4}$	126
Silicone oil	1	$1.34 \cdot 10^{-3}$	$6.25 \cdot 10^{-4}$	16.0
Water at 70°C	0.44	$6.09 \cdot 10^{-4}$	$1.62 \cdot 10^{-3}$	2.74

the critical value of 1707 at the rate of 1°C/min. After one or two time constants, the lamp is turned off, the grid is removed, and a set of convection rolls can be observed which have the wavelength and orientation of the grid. Because the shadowgraph visualization scheme was used, a depth of the oil was selected so as to reach the desired Rayleigh number with a temperature difference between top and bottom of 1–10°C.

Busse and Whitehead observed that a bandwidth of such rolls is stable to infinitesimal perturbations up to a Rayleigh number of 22,000, above which a second set of cross rolls commences to stably coexist with the original rolls. Since it was the intent of part of the present research to investigate the properties of this “bimodal flow,” the cross rolls were induced using a procedure similar to that used to induce the original rolls. Briefly, a grid with the desired cross-roll wavelength was placed at right angles to the original rolls while the system was kept at a Rayleigh number of 15,000, the lamp was turned on for an interval of one to two thermal time constants, the Rayleigh number was then increased to some value above 22,000 (usually 30,000), and finally the grid was removed, the lamp turned off, and the subsequent behavior of bimodal flow with controlled rolls and cross rolls was observed.

Observations were recorded by taking photographs at appropriate intervals, and in the cases of transition to oscillatory flow, time-lapse movies were taken at a speed of 8 frames/min. A time equivalent to at least two thermal time constants was allotted for any instabilities to begin to develop. If nothing was detected by the operator at this time, a value of “stable” was assigned. Naturally, it is impossible to determine stability completely by waiting an infinite time. Therefore it is possible that some of the data points which were reported stable would indeed be unstable if we were to wait longer. This might especially be the case for those data adjacent to the unstable region. However, our tendency was to wait longer than two time constants for those data, so as to clearly determine the transition, and therefore we believe that the data marked stable for two time constants are indeed stable forever.

The actual Rayleigh number in any experiment was not measured directly.

Based on the calculations on convective heat transport made by Busse (1967), for rolls, and based on measurements of heat transport by Rossby (1969), and Somerscales and Gazda (1969) of $Nu = 0.19 R^{0.282}$, and taking into consideration the finite conductivity of the glass boundaries, graphs relating the temperature difference in the two water channels (i.e., thermostat settings), with the Rayleigh number in the convection layer were obtained. The formula used was:

$$\Delta T_1 = \Delta T \left(1 + Nu \frac{k_1 d_2}{k_2 d_1} \right)$$

where ΔT_1 is temperature difference across the test fluid, ΔT is temperature difference between the baths, Nu is Nusselt number of fluid (a function of T_1), and k and d are thermal conductivity and thickness of the fluid (subscript 1) and glass (subscript 2) respectively. Such relationships are slightly non-linear, depending on the properties of the working fluid. The Rayleigh numbers deduced this way are accurate to approximately 10%. However, no great accuracy in their determination is required since these experiments are more qualitative than quantitative with respect to the Rayleigh number measurement.

STABILITY REGION OF ROLLS AT $Pr = 16$ AND 2.7

Stability region

The data from the experiments with the silicone oil are recorded graphically in Fig. 3. The balloon-shaped region correspond to the theoretically predicted stability region for a fluid, with $Pr = 16$, kindly supplied to us by R. Clever, using the technique of Busse (1967). In these experiments, the balloon shape of the stable region is generally conserved, except that it is shifted considerably to smaller wavenumbers. The same applies to the data from the experiments with hot water except that the shift is even more pronounced. This phenomenon may be accounted for by the finite conductivity of the glass boundaries which have the effect of lowering the critical wavenumber. A perturbation analysis shows that this effect is proportional to the product of the ratio of glass thickness to the convection-layer thickness and the inverse ratio of plate conductivity to fluid conductivity, that is, $d_P k_F / d_F k_P$ where the subscript P stands for plate and F stands for fluid. For Rayleigh numbers below 10,000 this quantity has the value of 0.052 for the silicone oil and 0.348 for the hot water. It is thus within expectation that a larger shift occurs in the hot water than in the silicone oil. In other words, the boundary conditions in the water experiments were more like constant heat flux than constant temperature. An analysis of these two kinds of boundary conditions, done by Sparrow et al. (1963) shows this effect.

In general, the present experiments confirm the statement that the Prandtl number has only a quantitative influence on finite-amplitude convection.

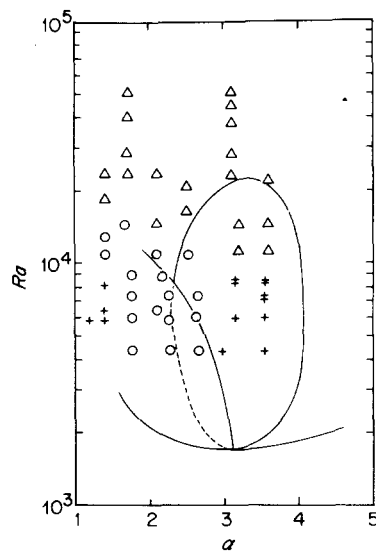
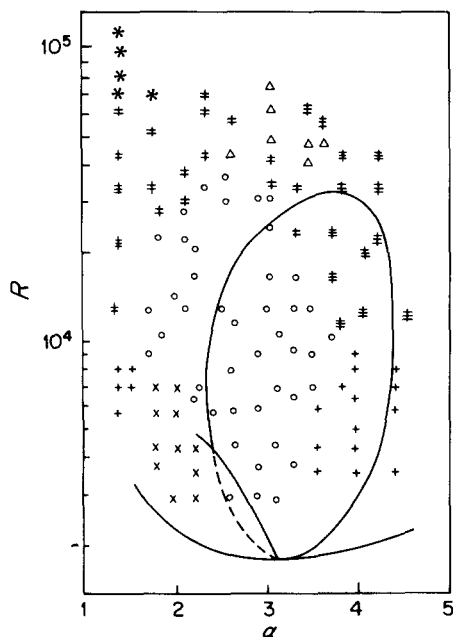


Fig. 3. Data for $Pr = 16$ experiments. \circ = stable rolls (no growth for two thermal constants); \times = zig-zag instability; $+$ = cross-roll instability; \ddagger = cross-roll instability leading to bimodal convection; $\#$ = cross-roll instability inducing transient rolls with subsequent local processes; $*$ = cross-roll instability leading to spokelike pattern (see pp. 45), Δ = see text. The curve was calculated by R. Clever using the technique of Busse, (1967), and kindly supplied to us.

Fig. 4. Data for hot-water experiments. \circ = stable rolls (no growth detected after two thermal time constants); $+$ = cross-roll instability; \ddagger = cross-roll instability leading to bimodal convection, Δ = see text pp. 42.

Instabilities

In the present experiments three kinds of instabilities were found. They are the zig-zag instability, the cross-roll instability, which leads to rolls, and another instability which leads to stationary three-dimensional convection. Experimental evidences seem to support the occurrence of these three kinds of instabilities at all Prandtl numbers.

It is clear from Fig. 3 that each of these three instabilities is responsible for a certain portion of the boundary of the stable region. In Busse and Whitehead (1971) an explanation was given for instabilities in convection rolls. They are basically to accomplish a transition from an unstable wavenumber to one that is stable, since the variational formulation of the linear problem indicates that there is a unique value α_c of the wave number at which the convection is optimally adjusted to the geometry of the layer.

The present discussion on the instabilities will be made with reference to the data for the $Pr = 16$ case. The data for hot water involves further complications

and will be examined later. The zig-zag instability is responsible for the lower left portion of the stable-region boundary; that is, it occurs at low Rayleigh numbers and small wavenumbers. In this range of wavenumbers the wavelengths of the rolls are too large compared to the optimal value. The rolls become wavy, with adjacent rolls perfectly in phase. This causes the wavelength of the rolls to be compressed. When the zigs and the zags are at right angles, they are disjoint at either the crests or the troughs, resulting in sets of rolls at about 45° to the original ones. It is impossible to obtain one complete set of new rolls at 45° to the original ones, since the probability of rolls of opposite orientation to occur is equal. The consequence is local regions of rolls oriented one way or the other at 45° . This instability was also clearly observed in hot water.

At large wavenumbers the cross-roll instability represents the emergence of a new set of rolls, perpendicular to the original ones. The wavelength of the cross rolls is independent of the wavelength of the original rolls. As the cross rolls grow, the original ones decay and finally disappear, thus accomplishing the transition to a smaller wavenumber. At Rayleigh numbers below 7000 the cross rolls become stable and persist. At Rayleigh numbers above this the transitions to cross rolls are followed by subsequent local processes which demolish the two-dimensionality of the convection pattern. This results in irregular patchy structures. Both of these two phenomena were also observed in hot water.

There is an intermediate range of wavenumbers at which the cross-roll instability at high Rayleigh numbers leads to stationary three-dimensional convection, otherwise called bimodal convection. In this case, although the cross rolls emerge in the same fashion as those previously described they bear a different meaning. Physically, as the cross rolls grow, the original rolls do not disappear. The two come into coexistence. As Busse (1967) has shown theoretically, above $R_2 = 22600$, two-dimensional rolls of all wavenumbers are unstable; it can be inferred that this cross-roll instability is a different physical mechanism than that which leads to rolls.

According to the regime diagram of Krishnamurti (1970b), bimodal convection is not expected to occur in hot water due to its low Prandtl number. However, a transition from steady to time-dependent flow is expected at a Rayleigh number near 9000. It should be the same kind of lateral oscillation of wavy rolls reported by Willis and Deardorff. The present experiments did not demonstrate it. What was observed in the hot-water experiments, represented by Δ data points in Fig. 4, is a zig-zag of rolls with a 180° phase difference in adjacent rolls. This mechanism always occurred in local patches, and not throughout the entire fluid, and also no critical Rayleigh number could be found below which it is not active, given enough time. Even in the silicone-oil experiments, the same was found, though much less active, in competition with other instabilities. Its apparent Prandtl-number dependence suggests that it is of a hydrodynamic cause rather than a convective cause, that is, it is linked to the nonlinear operator of the Navier–Stokes equation rather than the nonlinear operator of the heat equation.

STABILITY OF ARTIFICIALLY INITIATED BIMODAL FLOWS AT $Pr = 126$

Since an inherent characteristic of bimodal flow is two sets of rolls of different wavelengths at right angles, we will henceforth call the larger roll the original roll, with wavenumber α_1 , and the smaller roll the cross roll with wavenumber α_2 , where α is defined as $2\pi d/L$ where L is the roll wavelength and d is the depth of the fluid layer.

It was first desired to investigate the bandwidth of stable cross rolls as a function of Rayleigh number for a fixed value of the wavelength of the original roll. Fig. 5 shows such a stability curve for the fluid with a Prandtl number of 126 with α_1 fixed at 2.5. The bandwidth of stable α_2 was observed to increase with Rayleigh number. In the values of α_2 , reported stable in Fig. 5, the bimodal flows were observed to be stable for at least four thermal time constants after the experiment had reached a steady state. In those data close to the instability curve, it was evident that the amplitude of the cross rolls was very small because the shadowgraphs of the cross rolls were extremely faint. In the data denoted as unstable, the cross roll was observed to completely vanish from view. A new roll, with its wavenumber within the dashed lines, was then observed to appear. Such a sequence is shown in the three photographs comprising Fig. 6 for $\alpha_2 = 3.06$, $R = 26,000$. The final wavenumber is 3.9.

It was not possible to map out the entire volume of stable bimodal convection on the Rayleigh number, α_1 , α_2 volume due to practical limitations on experimental feasibility and time. Some stable regions in the R - α_1 plane are shown in Fig. 7. The data for this figure were obtained for fluid with a Prandtl number of 126, using a value of α_2 which the rolls selected as bimodal flow developed when Rayleigh number passed above 22,000 in a non-induced ex-

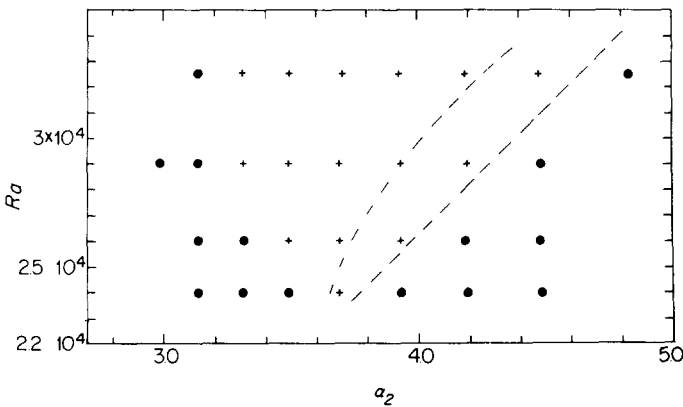


Fig. 5. Stability of the cross roll of wavenumber α_2 for bimodal flow with wavenumbers $\alpha_1 = 2.5$. $+$ = stable flows; \bullet = flows where the cross rolls decayed to an undetectable amplitude and cross rolls with a new value of α_2 emerged. The new value was always in the region between the dashed lines.

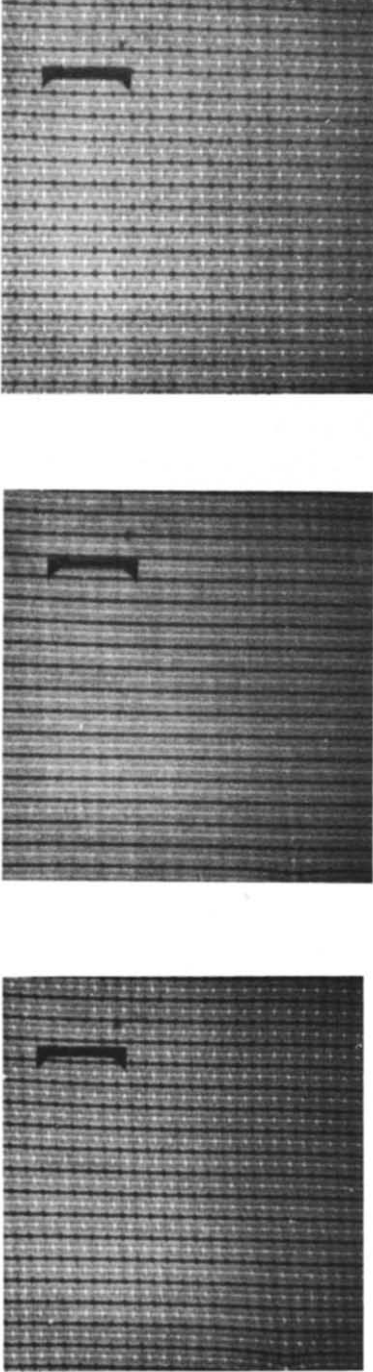


Fig. 6. Photographs of an unstable cross roll. $\alpha_1 = 2.54$, $\alpha_2 = 3.06$, $R = 26,000$. Dimensionless times $t\kappa/d^2$ are, respectively 0, 1.9, and 4.9 after the experiment reached the steady R . Final value of α_2 was 3.9.

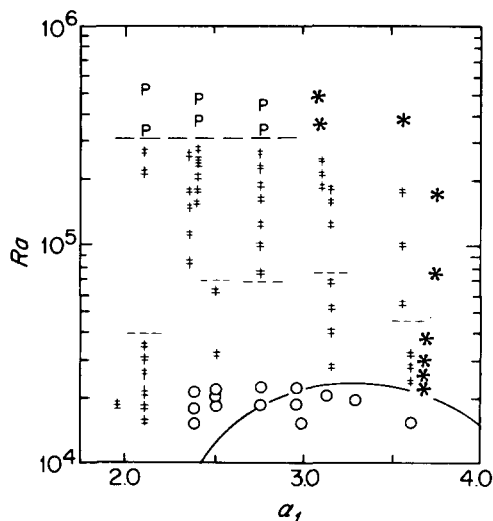


Fig. 7. Stability map of flawless bimodal flow. Data below the fine dashed lines are from Busse and Whitehead (1971). \circ = stable rolls (no growth detected after two thermal time constants); $+$ = stable bimodal flow, \ddagger and $*$ = unstable bimodal flow. Data above the heavy dashed line always oscillated, as denoted by P = oscillating bimodal flow.

periment. The data shown in Fig. 7 below the horizontal lightly dashed line are from Busse and Whitehead (1971). The data above the lightly dashed line were obtained in experiments in which rolls in both directions were induced with the above value of α_2 to insure uniformity of results.

The instabilities that arose when α_1 was too big or too small were the same as those described in Busse and Whitehead, and will be briefly reviewed here. If α_1 was too small, the roll with a size α_2 was observed to grow at the expense of the original roll, ultimately absorbing all energy, after which a new roll in the α_1 direction would grow to generate a bimodal flow in the stable region. This is denoted by a triple cross in Fig. 7 (more such instabilities are below the range of this graph). If α_1 was too large, a patchy, nonuniform, three-dimensional disturbance grew, which completely destroyed the uniform roll structure. This is denoted by an asterisk in Figs. 3 and 7.

When the Rayleigh number was above 300,000 the convection pulsed. This transition is dealt with more fully in Busse and Whitehead (1974).

STABILITY OF SPONTANEOUSLY APPEARING BIMODAL FLOW

The instability of the bimodal flow reported here at large Rayleigh number is so unlike the transitions to time-dependent convection reported by Krishnamurti at a Rayleigh number of 60,000 and Willis and Deardorff at Rayleigh number above 100,000, that it is important to clarify the cause of this paradox. In making the observations reported in the previous section, it was necessary to carefully control the wavelength and orientation of the bimodal flows because it was observed in preliminary experiments that this flow was extremely

sensitive to disruptions in its planform. The planform in the bimodal flow range which appears in the apparatus when the wavelengths are not artificially initiated, consists of a bimodal flow with disruptions or "flaws." These were always observed in places where neighboring rolls have trouble fitting together.

Photographs of such convection which grows from random initial conditions are shown in Fig. 8, arranged vertically. Each experiment was run sequentially

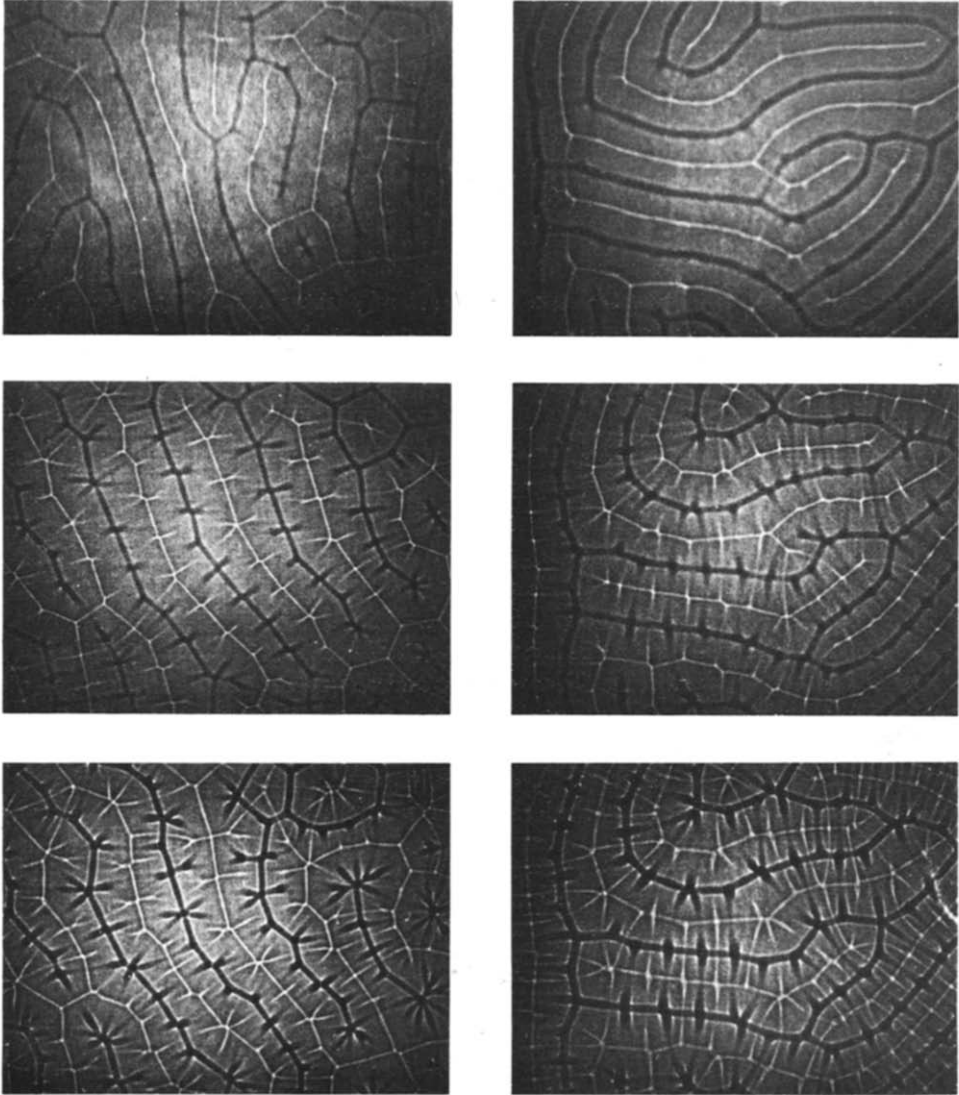


Fig. 8. Two sets of photographs arranged vertically of convection which has grown from random initial conditions. Top, roll convection with some bimodal convection, $R = 20,000$. Middle, bimodal convection, $R = 53,000$. Bottom, bimodal convection with some spoke-like convection, $R = 80,000$. Each photograph was taken 24 hours after the photograph above it.

at Rayleigh numbers of 20, 53, and 80 thousand, and each grew initially from a state of no motion, photographs being taken 24 hours after the temperature was set to new desired value. As Rayleigh number was increased, the disruption of the bimodal planform by these flaws increased until at a given value a new form of flow emerged at these flaws, as is evident at 80,000. For purposes of description here, we will call this new flow "spokelike" flow, as it appears to consist of a central spout of downwelling or upwelling fluid surrounded by spokelike sheets of fluid feeding into the spout. The spokelike flow invariably exhibited any oscillations that were present in the Rayleigh number range 40,000 to 100,000, and appears to be linked to the emergence of oscillations reported by Krishnamurti (1970b).

This flow was first observed at the pronounced "flaw" regions in the planform where two adjacent rolls fitted together poorly. At greater Rayleigh numbers, it was consistently observed that more and more spokelike flow existed as R increased. The estimated percentage of fluid in this flow is shown as a function of Rayleigh numbers in Fig. 9 for $Pr = 126$ and 16. The data were obtained by placing a transparent sheet of plastic over photographs of convection which had been allowed to occur spontaneously for a period of two hours, blacking over the regions with spokelike flow with a grease pencil, and then quantitatively determining the percentage of blacked-out area on the transparent sheet. The latter was done by shining parallel light through the transparency, by bringing this light to a focus with a convergent lens, and then by measuring the quantity of light at the focus with a calibrated photoresistor.

Fig. 9 shows that the relative amount of spokelike motion varies continuously from zero to 100%. This behavior is in contrast to the stability of a flawless bimodal flow, where the instabilities occur throughout the entire fluid region when the critical parameter is exceeded.

Structure of this spokelike flow was probed with a moveable thermocouple probe and recorded with movie and still cameras. In the still picture shown in Fig. 8, the most noticeable aspect of the new structure is the radial "spokes" of either black or white sheets of vertically convecting fluid. Temperature probe measurements indicate that the flow consists of three different regions:

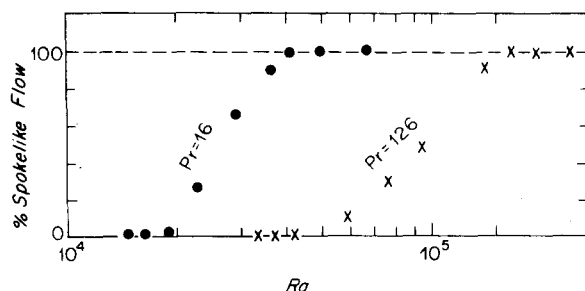


Fig. 9. Percentage of the flow field with a spokelike flow pattern as a function of Rayleigh number, R , for fluid with a Prandtl number of 126 (crosses) and 16 (solid circles).

(a) An unstable boundary layer at the top (or bottom) with vertical sheets of fluid continuously emitted from a thin unstable region, the sheets being aligned at right angles to the shear caused by downwelling in the interior

(b) A central downwelling (or upwelling) spout which entrains the fluid from the sheets by radial advection, the sheets in region (a) are aligned radially to this spout.

(c) A thin, quiet stagnation region at the bottom (or top) of the spout, which is characterized by no buoyant emissions. These spokelike regions were found to occur in about the same numbers with either sense, and were generally (but not always) accompanied by oscillations.

We note this ties in with a description given by Willis and Deardorff: "Unlike the case of air, the structure which first undergoes oscillations at large R and σ (Prandtl number) is not a long roll, but is an up- or down-draft segment having one end anchored to a more prominent up- or down-draft and the other end free." Lastly, movies made by Willis and Deardorff have been viewed and they look strongly like the time-lapse shadowgraph movies obtained in the present study.

We close this section by remarking that this spokelike flow and accompanying oscillations have been observed more fully and under more controlled conditions by Busse and Whitehead (1974).

CONCLUDING REMARKS

The biggest single difficulty in comparing these experimental results with others may seem to be the fact that glass only has conductivity a few times greater than silicon oil, while other experiments have metal boundaries above and below, with conductivity many hundreds of times greater than silicon oil. As evidence that supports the contention that the glass boundaries are a close approximation to perfect conductors, we first cite the agreement of the experiments here and in Busse and Whitehead (1971) with calculations of marginal stability and the finite-amplitude calculations of Busse (1967). Secondly, we cite the agreement of the appearance of oscillating spokelike flow in randomly oriented bimodal flow reported here with the observations of Krishnamurti (1970b). Indeed, differences in results only occurred when we induced a flawless planform. Thirdly, we point out that the glass is thinner than the silicon oil, so that in the large Rayleigh number experiments a measure of the finite conductivity of the boundary plate is $d_p k_F Nu / d_F k_p$, where k stands for conductivity, d stands for thickness, Nu stands for Nusselt number, and the subscripts p and F stand for plate and fluid, respectively. Using approximate values of $d_p = 0.6$, $k_F = 0.003$, $Nu = 4$, $d_F = 2$, and $k_p = 0.002$, (cgs units), which yield the greatest product in the silicon oil experiments, this number is 0.18.

It is clear that the picture of the various instabilities observed in the convection rolls in silicon oil with a Prandtl number of 16 closely resembles the picture of the instabilities of silicon oil with a Prandtl number of 126. In addition, the bimodal state appears to behave very much like the roll state as

Rayleigh number is progressively increased, showing an increasing amplitude and bandwidth in wavenumber space as the marginal state is left behind. This behavior is characteristic of a flow developing from a state which is unstable to infinitesimal instabilities. Unlike the rolls, the bimodal flow then develops a weakness to a transition to spokelike flow in the uncontrolled state which does not occur in the controlled state in the same parameter space. It does apparently occur in another region of parameter space (Busse and Whitehead, 1974). Quite possibly this spokelike planform requires a finite-amplitude perturbation before it can develop in this region, it certainly does not grow from background noise, and hence should not be predicted by a linearized stability analysis.

ACKNOWLEDGMENTS

The authors happily acknowledge many useful discussions with F. Busse. The apparatus was made by the late Paul Cox. Support was received from the National Science Foundation, Atmospheric Section, under grant nos. GA-849, GA-10167, and GA-19605, and Oceanography Section under grant no. GA-35447.

REFERENCES

- Bénard, H., 1901. Les tourbillons cellulaires dans une nappe liquide transportant de la chaleur par convection en régime permanent. *Ann. Chim. Phys.*, 23: 62–144.
- Busse, F.H., 1967. On the stability of two-dimensional convection in a layer heated from below. *J. Math. Phys.*, 46: 140–150.
- Busse, F.H. and Whitehead, J.A., 1971. Instabilities of convection rolls in high Prandtl number fluid. *J. Fluid Mech.*, 47: 305–320.
- Busse, F.H. and Whitehead, J.A., 1974. Oscillatory and collective instabilities in large Prandtl number convection. *J. Fluid Mech.*, 66: 67–80.
- Chen, M.M. and Whitehead, J.A., 1968. Evolution of two-dimensional periodic Rayleigh convection cells of arbitrary wavenumbers. *J. Fluid Mech.*, 31: 1–15.
- Krishnamurti, R., 1970a. On the transition to turbulent convection, 1. The transition from two- to three-dimensional flow. *J. Fluid Mech.*, 42: 295–307.
- Krishnamurti, R., 1970b. On the transition to turbulent convection, 2. The transition to time dependent flow. *J. Fluid Mech.*, 42: 309–320.
- Malkus, W.V.R., 1954. The heat transport and spectrum of thermal turbulence. *Proc. R. Soc. London, Ser. A*, 225: 196–212.
- Rossby, H.T., 1969. A study of Bénard convection with and without rotation. *J. Fluid Mech.*, 36: 309–335.
- Somerscales, E.F.G. and Gazda, I.W., 1969. Thermal convection in high Prandtl number liquids at high Rayleigh numbers. *Int. J. Heat Mass Transfer*, 12: 1491–1511.
- Sparrow, E.M., Goldstein, R.J. and Jonsson, V.K., 1963. Thermal instability in a fluid layer, the effect of boundary conditions and non-linear temperature profile. *J. Fluid Mech.*, 18: p. 513.
- Willis, G.E. and Deardorff, J.W., 1970. The oscillatory motions of Rayleigh convection. *J. Fluid Mech.*, 44: 661–672.